

# A potential linkage between excess silicate-bound nitrogen and N<sub>2</sub>-rich natural gas in sedimentary reservoirs

Yang Liu<sup>a, b\*</sup>, Eva E. Stüeken<sup>c</sup>, Dongsheng Wang<sup>a, b</sup>, Xuan Tang<sup>a, b</sup>, Haikuan Nie<sup>d</sup>, Wei Dang<sup>e</sup>, Jinchuan Zhang<sup>a, b</sup>

<sup>a</sup> School of Energy resource, China University of Geosciences (Beijing), Beijing 100083, China.

<sup>b</sup> Key Laboratory of Strategy Evaluation for Shale Gas of Ministry of Land and Resources, China University of Geosciences (Beijing), Beijing, 100083, China.

<sup>c</sup> School of Earth and Environmental Sciences, University of St. Andrews, St. Andrews KY16 9AL, United Kingdom.

<sup>d</sup> Petroleum Exploration and Production Research Institute, SINOPEC, Beijing 100083, China.

<sup>e</sup> School of Earth Sciences and Engineering, Xi'an Shiyou University, Xi'an 710065, China.

Corresponding Author: [yangliu@cugb.edu.cn](mailto:yangliu@cugb.edu.cn)

## Abstract

Molecular nitrogen (N<sub>2</sub>) released from sedimentary rocks during metamorphism is an important component of the biogeochemical nitrogen cycles. However, the importance and variability of this metamorphic N<sub>2</sub> flux from rock nitrogen to Earth's surface environment remains largely unexplored. Here we present a comprehensive bulk rock C-N and N<sub>2</sub> concentration dataset from the lower Cambrian shale across the Yangtze Block. The results reveal a spatial trend of excess silicate-bound nitrogen in the lower Cambrian shale throughout the Yangtze Block, which is interpreted as partial assimilation of ammonium (NH<sub>4</sub><sup>+</sup>) with high concentrations of NH<sub>4</sub><sup>+</sup> accumulating in the euxinic water column and in sediment pore waters at shelf and slope environments during sedimentation. The remarkable spatial coupling between silicate-bound nitrogen in bulk rock shale and N<sub>2</sub> concentration in modern shale reservoirs indicates that the high proportion of silicate-bound nitrogen may act as an important control on the formation of N<sub>2</sub>-rich gas in shale reservoirs during metamorphism. These N<sub>2</sub>-rich reservoir rocks may have affected the surface environment through tectonic movement over Earth's history. Our results therefore identify a novel linkage in the nitrogen cycle and provide evidence for the importance of metamorphism on the return of rock nitrogen back to the surface environment. We further reveal that the metamorphic N<sub>2</sub> gas flux from the geosphere to the atmosphere is dependent on environmental conditions during sediment deposition.

**Key words:** Nitrogen cycling; N<sub>2</sub>-rich natural gas; Silicate-bound nitrogen; Early Cambrian; Yangtze Block.

# 1. Introduction

## 1.1. Unanswered questions about metamorphic N<sub>2</sub> gas release

Nitrogen (N) is one of the essential constituents of life and serves as a limiting nutrient affecting biological evolution in the oceans on geological timescales (Anbar and Knoll, 2002; Canfield et al., 2010; Stüeken et al., 2016). In the form of molecular N<sub>2</sub> gas, nitrogen is the most abundant constituent of the Earth's atmosphere. Another large nitrogen reservoir is the continental crust, including ancient sedimentary rocks, which holds roughly half as much nitrogen as the atmosphere (Johnson and Goldblatt, 2015). Most nitrogen in rocks is bound to organic matter and minerals in the form of ammonium. The nitrogen reservoirs of the atmosphere and geosphere are linked, because nitrogen can be buried in sediments along with clays and biomass, and it can be released from rocks into surface environments during weathering and metamorphism (Canfield et al., 2010; Stüeken et al., 2017; Houlton et al., 2018). The geological nitrogen cycle thus shares similarities with the carbon cycle in that both are strongly affected by the burial and post-depositional alteration of biomass; however, the behavior of silicate- and organic-bound nitrogen relative to organic carbon during thermal maturation of organic matter to natural gas is not well explored.

Molecular nitrogen is one of the most common non-hydrocarbon compounds in natural gas reservoirs, and generally only a few percent (mostly < 4%) of N<sub>2</sub> is present in most conventional natural gas reservoirs around the world (Jenden et al., 1988; Dai, 1992). However, high concentrations of N<sub>2</sub> have long been known in some conventional hydrocarbon reservoirs, such as the North German Basin (greater than 90%, Littke et al., 1995), the Tarim Basin (up to 50%, Liu et al., 2012) and the Great Valley basin (up to 87%, Jenden et al., 1988). Recently, widespread occurrence of N<sub>2</sub>-rich gas (up to 95%) in the lower Cambrian shale reservoirs on the Yangtze Block (South China) was reported (Liu et al., 2016; Li et al., 2020; Gai et al., 2020). Such N<sub>2</sub>-rich gas is worthless from a commercial point of view and therefore constitutes a serious exploration risk in many petroliferous basins (Littke et al., 1995; Liu et al., 2012). However, the large nitrogen quantities released from these sedimentary reservoirs may have played a previously underestimated role in maintaining the atmospheric N<sub>2</sub> budget. A recent study revealed that the degassing flux of the crust and mantle is unbalanced with the transfer of nitrogen from the ocean to the crust (Houlton et al., 2018). The maintenance of the atmospheric nitrogen reservoir thus requires a transfer of additional nitrogen from crustal rocks to the surface environment, and rock nitrogen weathering was identified as a considerable atmospheric nitrogen input (Houlton et al., 2018). Here we propose that another previously neglected nitrogen source to the atmosphere is degassing of N<sub>2</sub> from sedimentary reservoirs independently from hydrocarbons. Further characterizing the origin of this N<sub>2</sub> gas from sedimentary reservoirs is therefore of great significance for understanding the balance of the Earth's nitrogen budget.

Numerous studies have been conducted on the origin and enrichment mechanism of N<sub>2</sub>-rich natural gas (e.g., Littke et al., 1995; Zhu et al., 2000; Liu et al., 2016). The N<sub>2</sub> generated from sedimentary organic matter at high temperatures (i.e., high thermal maturity of organic matter) and atmospheric nitrogen input are considered to be the two most important sources of N<sub>2</sub> in sedimentary reservoirs (Krooss et al., 1995; Boudou and Espitalié, 1995; Littke et al., 1995; Huang et al., 2019; Gai et al., 2020). However, this model has shown limitations in explaining

the differential accumulation of N<sub>2</sub> in the lower Paleozoic shale reservoirs in South China. Compared with the unusually N<sub>2</sub>-rich gas from the lower Cambrian shale of the Yangtze Block, the gas generated from another set of overmature marine shale of Ordovician–Silurian age in the same region does not show a high content of N<sub>2</sub> (Dai et al., 2014; Nie et al., 2021), even in the areas where the two sets of shales have experienced similar tectonic deformation and thermal maturity levels (Gai et al., 2020). Recent studies (Chen et al., 2019; Liu et al., 2020) have reported the presence of excess silicate-bound nitrogen in the lower Cambrian shale on the Yangtze Block, which coincides with the widespread N<sub>2</sub>-rich gas in the same shale reservoir. In light of this potential linkage, the present study aimed (1) to investigate the degree and distribution of excess silicate-bound nitrogen in lower Cambrian shale throughout the Yangtze Block; (2) to decipher the origin and spatial variability of excess silicate-bound nitrogen in lower Cambrian shale; and (3) to explore the possible links between excess silicate-bound nitrogen in bulk rocks and N<sub>2</sub>-rich gas in the lower Cambrian shale reservoirs. We will use nitrogen isotopes of bulk rocks to explore if the N<sub>2</sub>-gas enrichments may be linked to primary biogeochemical processes during the time of sedimentation.

### **1.2. An overview of nitrogen isotope fractionation pathways**

Nitrogen isotopes ( $\delta^{15}\text{N}$  values) can provide valuable information about the redox state of the ocean and have been widely used for reconstructing nitrogen cycling in modern and ancient environments (reviewed by Stüeken et al., 2016). In the modern oceans, bioavailable nitrogen enters the marine system mainly through biological fixation of atmospheric N<sub>2</sub> (N<sub>2</sub>-fixation) with a small isotopic fractionation ( $\epsilon \approx \delta^{15}\text{N}_{\text{product}} - \delta^{15}\text{N}_{\text{reactant}}$ ) of  $-1\text{‰}$  on average (range from  $-2\text{‰}$  to  $+1\text{‰}$ ). However, this fractionation can be as large as  $-4\text{‰}$  under Fe<sup>2+</sup>-rich or thermophilic conditions (e.g., Zerkle et al., 2008; Zhang et al., 2014). When organisms die, the organic N is converted to NH<sub>4</sub><sup>+</sup> through ammonification with negligible isotopic fractionation. Under oxic conditions, the NH<sub>4</sub><sup>+</sup> released during organic matter degradation is rapidly oxidized to nitrite (NO<sub>2</sub><sup>-</sup>) and subsequently to nitrate (NO<sub>3</sub><sup>-</sup>) through nitrification, also with negligible fractionation because nitrification is typically rapid and quantitative (Sigman et al., 2009). Assimilation of NO<sub>3</sub><sup>-</sup> imparts an isotopic fractionation of  $-5\text{‰}$  to  $-10\text{‰}$ , but these fractionations are generally not expressed because NO<sub>3</sub><sup>-</sup> assimilation typically goes to completion (Altabet and Francois, 1994). Under anoxic conditions, denitrification and anammox are two major pathways of N loss (NO<sub>3</sub><sup>-</sup>, NH<sub>4</sub><sup>+</sup> and NO<sub>2</sub><sup>-</sup> are converted into gaseous species NO<sub>2</sub> or N<sub>2</sub>) from the ocean. The isotopic fractionation of both processes is around  $-5\text{‰}$  to  $-30\text{‰}$  in the water column, but negligible in the sediments (Sigman et al., 2009; Lam et al., 2009; Lam and Kuypers, 2011). Incomplete assimilation of NH<sub>4</sub><sup>+</sup> imparts large isotopic fractionations of  $-4\text{‰}$  to  $-27\text{‰}$ , depending on ambient NH<sub>4</sub><sup>+</sup> concentrations. The  $\delta^{15}\text{N}$  composition of sedimentary rocks can therefore provide insights into the aqueous nitrogen cycle during deposition.

## **2. Material and Methods**

### **2.1. Geological setting and samples**

The South China Craton is composed of the Yangtze and Cathaysia Blocks. The Yangtze Block preserves marine sedimentary rocks spanning from the Neoproterozoic to the Ordovician.

Paleogeographic reconstructions suggest that three broad paleoenvironmental settings were developed on the Yangtze Block during the Ediacaran to early Cambrian period, including platform facies to the northwest, a transition zone in the central region and deep-water slope/basin facies to the southeast (Steiner et al., 2007; Zhu et al., 2007; Fig. 1). During Cambrian Stage 2 to early Stage 3, a major marine transgression resulted in the deposition of organic-rich shales over the entire Yangtze Block (Zhu et al., 2003; Steiner et al., 2007; Jiang et al., 2012). These widely distributed organic-rich shales are characterized by great thickness (50–200 m) and a relatively high degree of thermal maturation, indicating a good gas-bearing potential and shale gas exploitation prospects (Wang, 2018; Zhao et al., 2019; Li et al., 2020).

Our studied drill core samples (forty-two) for bulk rock C-N analysis were taken from the CY 1 well, which is located in the eastern Guizhou Province, South China, and paleogeographically lies in the slope of the Yangtze Block. The CY 1 well preserves a relatively continuous record from the late Ediacaran to Cambrian Series 2, and consists of the Liuchapo, Jiumenchong and Bianmachong Fms., in ascending order. Twenty-four lower Cambrian shale samples for X-ray diffraction (XRD) analysis were collected from different areas of the Yangtze Block, including five core samples and nineteen outcrop samples. Natural gas samples for N<sub>2</sub> concentration analysis were obtained from seventeen shale gas wells on the Yangtze Block (Fig. 1).

## 2.2. Analytical methods

Prior to bulk rock geochemical analysis, approximately 300–500 g of each bulk sample was carefully trimmed to avoid veins and potential weathered surfaces, and remaining material was powdered using an agate mortar.

Total organic carbon (TOC), total nitrogen (TN) and nitrogen isotopic analysis was conducted at the State Key Laboratory of Biogeology and Environmental Geology (BGEG) of the China University of Geosciences, Wuhan. Detailed descriptions of these methods can be found in Du et al. (2021). Prior to analysis, sample powders were decarbonated using 3 mol/L HCl at room temperature for 24 h. Residues were then rinsed with 18.2 MΩ/cm deionized water to remove the acid and subsequently dried at 45 °C overnight. TOC and TN concentrations were measured on decarbonated samples using a Vario Macro Cube elemental analyzer (Elementar, Hanau, Germany) at BGEG. The analytical uncertainties of TOC and TN contents were better than 0.05 wt% based on replicate analyses of multiple samples. Nitrogen isotope compositions were measured using a Flash HT 2000 Plus and continuous-flow Delta V Advantage IRMS (Thermo Fisher Scientific) at BGEG. Briefly, 40–80 mg of decarbonated samples were mixed with V<sub>2</sub>O<sub>5</sub> and sealed in a tin capsule and combusted at 1020 °C, and the simultaneously generated CO<sub>2</sub> in the outflow gas mixture was absorbed by an alkali lime trap. Nitrogen isotope results are reported using standard  $\delta$  notation in per mil (‰) deviations from atmospheric N<sub>2</sub> ( $\delta^{15}\text{N} = 0\text{‰}$ ). Two international standards USGS40 ( $\delta^{15}\text{N} = -4.52\text{‰}$ ) and IAEA-N-2 ( $\delta^{15}\text{N} = +20.3\text{‰}$ ) were used for  $\delta^{15}\text{N}$  calibration and the standard deviation of replicate analyses was better than 0.3%.

Chemical compositions of natural gas were measured using an Agilent 6890N gas chromatograph (GC) equipped with a flame ionization detector and a thermal conductivity detector, following the procedures described in Liu et al. (2016). The GC oven temperature was initially set at 30 °C for 10 min and then ramped to 180 °C at a rate of 10 °C/min, and held at

this temperature for 20–30 min. The average analytical precision was  $\pm 1\%$ .

X-ray diffraction (XRD) analysis of shale powders was performed on a Bruker D8 Advance X-ray diffractometer at 40 kV and 30 mA with Cu K $\alpha$  radiation ( $\lambda=1.5406$  for CuK $\alpha$ 1). Stepwise scanning measurements were performed at a rate of 4°/min in the range of 3–85° (2 $\theta$ ). The relative mineral proportions were estimated based on the areas of their major peaks with Lorentz polarization correction (Pecharsky and Zavalij, 2003).

### 3. Results

#### 3.1. Bulk rock carbon and nitrogen data

The TOC, TN and  $\delta^{15}\text{N}$  data from our samples (CY 1 well), paired with compilations from the literatures, provide information from twenty-two sections across the Yangtze Block (Fig. 1), representing shallow to deep marine environments (Table S1), which span the entire Fortunian to Cambrian Stage 3 (~540–515 Ma), including the target intervals of organic-rich shales for early Cambrian shale gas exploration (~526–515 Ma; Gao et al., 2021). The organic-rich shale deposited during this time period on the Yangtze Block exhibits high TOC values (0.03–31.28 wt%, mean = 4.36 wt%; Fig. 4b), and is therefore considered to be a high-quality source rock for conventional and unconventional hydrocarbons (Zou et al., 2015; Gao et al., 2021). The correlation between TOC and TN of the lower Cambrian source rocks from platform to slope environment yields a significant positive intercept on the TN-axis. This positive N-intercept gradually rises from 665 ppm on the platform to 955 ppm on the shelf, with a maximum on the slope (2046 ppm), but only a minor N-intercept (32 ppm) is observed in the basal environment (Fig. 3). The bulk rock TN/TOC ratios during the ~540–526 Ma interval are mostly around 0.01 to 0.02. However, the TN/TOC ratios of samples from the shelf and slope environments exhibit a positive shift toward high values of 0.03 to 0.50 during the ~526–515 Ma (Fig 4c). The  $\delta^{15}\text{N}$  values from the Cambrian Fortunian to early Stage 2 (~540–526 Ma) vary between +1‰ and +9‰. Subsequently, a negative shift occurs at most sections (most values vary between –2‰ and +1‰) with very low  $\delta^{15}\text{N}$  values below –4‰ at the shelf and slope sections during Cambrian Stage 2 (~526–521 Ma). Although the  $\delta^{15}\text{N}$  values increase to different extents (from –2‰ to +6.9‰, with most values are between 0‰ and +3‰) at most sections during Cambrian Stage 3 (~521–515 Ma), some anomalously negative  $\delta^{15}\text{N}$  values (< –2‰) are still recorded in the slope sections (Fig. 4d).

#### 3.2. X-ray diffraction

The samples we measured from various sedimentary environments across the Yangtze Block have similar mineralogical compositions. The X-ray diffraction results (Table S2) show that the lower Cambrian shales are dominated by quartz (mostly in the range of 40–60%, mean = 51%) and clays (mainly between 20% to 40%, mean = 30%). The clay minerals are dominated by illite and illite/smectite mixed-layer (I/S), and the illite + I/S contents range between 11% and 46%, with a mean value of 27%. Furthermore, the illite + I/S contents in samples from different sedimentary environments show limited variability.

#### 3.3. Gas compositions

Gas composition data from twenty-six shale gas wells (seventeen from this study and nine

from literatures, Fig. 1) across the Yangtze Block show highly variable N<sub>2</sub> concentrations (0.03–97.45%; Table S3) in the lower Cambrian shale reservoirs. The N<sub>2</sub> concentrations show a similar spatial trend to the TN excess in the lower Cambrian shale across the Yangtze Block, which gradually rises from the platform (27.90–45.16%, mean = 36.53%) to the shelf (25.00–87.89%, mean = 62.06%) and slope (76.00–97.45%, mean = 89.25%), with the minimum in the basin (0.03–29.20%, mean = 15.23%) setting.

## 4. Discussion

### 4.1 Evaluation of nitrogen isotope values

Sedimentary nitrogen budget and associated  $\delta^{15}\text{N}$  values may be modified by burial diagenesis and metamorphic alteration (reviewed by Ader et al., 2016; Stüeken et al., 2016). For instance, there is only a minor isotopic fractionation (< 1‰) imparted during diagenesis under anoxic conditions (Altabet et al., 1999; Thunell et al., 2004). However, oxic diagenesis can result in an increase in  $\delta^{15}\text{N}$  values by ~ 4‰ (e.g., Altabet et al., 1999; Freudenthal et al., 2001). In terms of metamorphism, the alteration of  $\delta^{15}\text{N}$  values is negligible (< 1‰) below greenschist facies, and minor (1 – 2‰) within the greenschist facies (reviewed by Ader et al., 2016; Stüeken et al., 2016). Hence, the  $\delta^{15}\text{N}$  values in sedimentary rock requires careful evaluation to ascertain whether the nitrogen isotopic data are reliable and record primary marine signals.

Multiple lines of evidence argue against a significant secondary alteration of the  $\delta^{15}\text{N}$  values in our samples from drill core CY1. First, published Fe-speciation data throughout the Yangtze Block suggest that the continental shelf and slope sediments were deposited under a persistently anoxic water column conditions during Cambrian Stage 2 to Stage 3 (Li et al., 2017), and thus the isotopic alteration during early diagenesis would have been minimal. Second, the thermal maturity and H/C ratio of organic matter in the lower Cambrian black shale indicate that these rocks are well below the greenschist facies (Křibek et al., 2007), suggesting negligible isotopic alteration during metamorphism. Third, the lack of correlation between  $\delta^{15}\text{N}$  values and TOC, TN or C/N ratios (Fig. 2) suggest that even if some nitrogen was mobilized and redistributed between organic matter, minerals and fluid phases during diagenesis and metamorphism, bulk rock  $\delta^{15}\text{N}$  values were probably not been significantly altered. Thus, the  $\delta^{15}\text{N}$  values recorded in our samples likely represent near-primary compositions.

### 4.2 Excess silicate-bound nitrogen across the Yangtze Block

Sedimentary nitrogen mainly occurs in organic-bound (bound to kerogen) and silicate-bound (mostly clay minerals) phases (Stüeken et al., 2017). In organic-rich sediments, most nitrogen is initially organically bound because it was buried together with the biomass of living organisms (Stüeken et al., 2017). During burial diagenesis of the sediments, ammonium ( $\text{NH}_4^+$ ) can be liberated into sediment pore waters where it can reach mM concentrations (e.g., Boudreau and Canfield, 1988). The released  $\text{NH}_4^+$  can then adsorb to clay minerals (e.g., illite) and become incorporated into their crystal lattice in substitution for  $\text{K}^+$  (Müller, 1977; Schroeder and McLain, 1998). Diagenetic degradation of organic matter typically leads to preferential loss of N over carbon, because N-rich compounds such as DNA and peptides are degraded more rapidly (Abdulla et al., 2018). However, if organic matter is partially degraded

by sulfate-reducing organisms during diagenesis or in the water column, then this can lead to accumulation of  $\text{NH}_4^+$  in excess of organic carbon, because the latter is converted to  $\text{CO}_2$  or  $\text{CH}_4$  while  $\text{NH}_4^+$  stays behind (Stüeken et al., 2016). Such an excess of silicate-bound ammonium is commonly reflected in a positive TN-intercept of the linear regression of TN versus TOC (e.g., Fulton et al., 2012; Chen et al., 2019). For example, sediments from the modern Black Sea display an intercept of 575 ppm (Fulton et al., 2012), reflecting accumulation of excess  $\text{NH}_4^+$  in euxinic (anoxic and sulfidic) bottom waters, while open marine sediments from the Atlantic Ocean have on average less than 50 ppm TN excess (Muzuka and Hillaire-Marcel, 1999; Li and Bebout, 2005). The relatively high TN intercepts in some of our sample sets are therefore a good indicator for the presence of a significant  $\text{NH}_4^+$  reservoir that accumulated under anoxic conditions and got trapped in clay minerals. The TOC–TN correlations for shales from platform to slope successions show a weak positive correlation (Fig. 3), indicating perhaps variable loss of nitrogen from the organic fraction, which may have weakened this correlation.

An alternative mechanism for positive TN-intercept is input of detrital clay minerals that are enriched in N. However, in our case, the TN-intercepts increase from nearshore platform to offshore slope, which is contrary to the trend expected from the distance from the continent, indicating that the excess silicate-bound nitrogen was not sourced from terrestrial input. We can also rule out that the excess TN in our samples was derived from diagenetic influx of  $\text{NH}_4^+$ , which was recently documented for organic-lean bentonites (Koehler et al., 2019). The Cambrian strata investigated in this study are dominated by organic-rich shale and argillaceous siltstone with higher TOC values than adjacent strata (e.g., Gao et al., 2021; Fig. 4b). Hence there are no plausible source rocks for external  $\text{NH}_4^+$  input. Lastly, another possible contribution to excess TN abundances in sedimentary rocks is biological production of ammonium from nitrate during sediment deposition (DNRA, dissimilatory nitrate reduction to ammonium), which can occur in sediments and in the water column (Sørensen, 1978; Kartal et al., 2007), preferably under ferruginous (anoxic and iron-rich) conditions (Michiels et al., 2017). We cannot appraise the relative contribution of this metabolism, but in any case, it would further support our conclusion of a significant ammonium reservoir that accumulated in anoxic waters and led to excess amounts of trapped N in clays.

The high proportion of silicate-bound nitrogen fraction in the lower Cambrian shales is further supported by the TN/TOC ratios of bulk rocks compared to kerogen extracts. Early studies have shown that the TN/TOC ratio of coal or kerogen of similar thermal maturity is mostly in the range of 0.01 to 0.02 (Littke et al., 1995; Jurisch et al., 2012; Gai et al., 2020). Thus, the elevated bulk rock TN/TOC ratios ( $> 0.01$ – $0.02$ ; Figs. 3 and 4c) for the lower Cambrian shales (platform to slope environment) indicate a significant contribution of silicate-bound nitrogen. A recent study (Gai et al., 2020) has illustrated that the bulk rock TN/TOC ratio of lower Cambrian shale (0.0787) was significantly higher than that of Ordovician–Silurian shale (0.0463) and Mesoproterozoic shale (0.0466), but similar TN/TOC ratios were found in their kerogen isolates (0.0188, 0.0162 and 0.0196, respectively), suggesting that the lower Cambrian shale contains significantly higher silicate-bound nitrogen than those of the other two shale formations. Paired with the significant positive TN-intercept observed in the lower Cambrian shales and the absence of this intercept ( $\sim 0$  ppm) from shales across the Ordovician–Silurian transition (e.g., Luo et al., 2016), our data thus provide evidence for higher

silicate-bound nitrogen fraction in the lower Cambrian shale, and this was most likely derived from a relatively high dissolved ammonium concentration in anoxic pore waters during diagenesis.

### 4.3 Origin of excess silicate-bound nitrogen

Our C-N dataset thus provide indirect evidence for anoxic pore waters across the Cambrian Yangtze Block. This scenario is supported by the redox landscape (Fig. 4a) of the early Cambrian ocean (~540–515 Ma), which has been well documented in previous studies (e.g. Jin et al., 2016; Li et al., 2017; Liu et al., 2020). During the Cambrian Stage 2 to early Stage 3, the widespread euxinic waters were dynamically maintained on the shelf and slope environment with a shallow chemocline and intermittent photic zone euxinia. Such euxinic conditions should have been conducive to ammonium accumulation, similar to the modern Black Sea (Brewer and Murray, 1973). This excess amount of  $\text{NH}_4^+$  is further supported by the anomalously negative  $\delta^{15}\text{N}$  values ( $< -2\text{‰}$ ), which are mostly observed in samples from the shelf and slope environment throughout Cambrian Stage 2 – 3 (Fig. 4d). During Cambrian Stage 3, a shift of  $\delta^{15}\text{N}$  to more positive values recorded in the shallow platform environment likely indicates increased nitrate availability in more oxic shallow waters (Liu et al., 2020). The negative  $\delta^{15}\text{N}$  signals observed during this time period have previously been interpreted as partial  $\text{NH}_4^+$  assimilation by organisms, leading to incomplete utilization of  $\text{NH}_4^+$  (Wang et al., 2018; Chen et al., 2019; Liu et al., 2020). For this to occur, the  $\text{NH}_4^+$  concentration in the water column may have reached ~30  $\mu\text{M}$ , below which the isotopic fractionation is not well expressed (Hoch et al., 1992). But it could easily have been higher within sedimentary pore waters, where modern anoxic sediments show millimolar levels (e.g., Boudreau and Canfield 1988). The excess  $\text{NH}_4^+$  in the anoxic pore waters could then be captured by clay minerals, resulting in the significant positive N-intercepts observed at the shelf and slope facies (Fig. 5a). Indeed, our X-ray diffraction (XRD) results (Table S2) of the lower Cambrian shale across the Yangtze Block show a high abundance (11–46%, mean = 27%; Fig. 5a) of illite + I/S (illite/smectite mixed-layer), which has been shown to take up  $\text{NH}_4^+$  into their crystal lattice (Schroeder and McLain, 1998; Koehler et al., 2019).

In contrast, the negligible positive N-intercept and strong TOC–TN correlations in sediments from the basinal environment (Fig. 3) suggests that  $\text{NH}_4^+$  may not have accumulated significantly in anoxic basinal environments. The lack of excess silicate-bound nitrogen in the basinal environment could perhaps be attributed to the lower illitic clay contents in shales deposited in these settings relative to shelf and slope environment. However, this scenario is not supported by the available XRD data of the lower Cambrian shale (Table S2), which shows that the basinal samples ( $26 \pm 3\%$ ) have similar illite + I/S contents to the shelf ( $29 \pm 9\%$ ) or slope ( $26 \pm 8\%$ ) samples. Furthermore, an investigation of positive N-intercept between different lithologies in the lower Cambrian strata suggests a limited role of clay content in the excess silicate-bound nitrogen. Alternatively, the low proportion of silicate-bound nitrogen in the basinal environment may reflect the limited accumulation of  $\text{NH}_4^+$  in pore waters, which is linked to the extent of organic matter remineralization during diagenesis. Unlike extensive euxinic conditions in shelf and slope environments, the basinal environments remained largely ferruginous throughout Cambrian Stage 2 – 3 (e.g., Jin et al., 2016; Li et al., 2017; Liu et al., 2020), possibly due to limited sulfate supply in deep waters (Feng et al., 2014). In this case,

organic matter remineralization and sulfate reduction would have been weakened, thus reducing the release of  $\text{NH}_4^+$  from organic matter into pore waters. In addition, due to the lower deposition rate in the basinal environment, even if some  $\text{NH}_4^+$  was released during the organic matter remineralization, it would be expected to have occurred in the water column or at the surface sediment, thus preventing  $\text{NH}_4^+$  accumulation in the pore waters. The degradation of organic matter in the water column may have resulted in preferential loss of nitrogen against carbon (Knauer et al., 1979), lowering the TN/TOC ratios in the sediment as we observed in basinal samples (Fig. 4c).

In terms of the Ordovician–Silurian organic-rich shales, which generally have similar mineralogical compositions and thermal maturity levels to the lower Cambrian shales (Wang, 2018; Gai et al., 2020; Nie et al., 2021). A recent compilation of  $\delta^{15}\text{N}$  data suggests a widespread limitation of fixed nitrogen in the late Ordovician-early Silurian ocean, with no evidence of partial  $\text{NH}_4^+$  assimilation (Koehler et al., 2019). This suggests that the concentration of  $\text{NH}_4^+$  in the water column and pore waters may not have accumulated to high levels during this period, leading to the absence of positive TN-intercept in Ordovician–Silurian shales. The significant differences in silicate-bound nitrogen abundance and  $\delta^{15}\text{N}$  records between Ordovician–Silurian and lower Cambrian shales further support our view that the marine nitrogen cycle in the early Cambrian ocean may have controlled the excess silicate-bound nitrogen in the lower Cambrian shales.

#### **4.4 Metamorphic $\text{N}_2$ flux from rocks to gas reservoir and surface environments**

During burial diagenesis and catagenesis, carbon and nitrogen in sedimentary rocks would be lost and converted into hydrocarbons and nitrogen gases, respectively, through thermal and chemical degradation (Behar et al., 2000; Boudou et al., 2008; Gai et al., 2020). Previous studies have suggested several possible sources of  $\text{N}_2$  in the lower Cambrian shale reservoirs on the Yangtze Block, including atmospheric nitrogen (Huang et al., 2019; Wang et al., 2020) and decomposition of sedimentary organic matter and/or clay minerals (Liu et al., 2016; Gai et al., 2020). The atmospheric origin seems unlikely, because another set of Ordovician–Silurian organic-rich shales on the Yangtze Block does not show a high concentration of  $\text{N}_2$  (lower than 2.2% on average; Dai et al., 2014). Indeed, early pyrolytic studies have shown that thermal degradation of nitrogen species in sedimentary rocks plays an important role in  $\text{N}_2$  accumulation in natural gas reservoirs; specifically, it was found that  $\text{N}_2$  is mainly generated at the final stage of gas generation after methane generation is practically exhausted (Krooss et al., 1995; Littke et al., 1995; Heim et al., 2012; Jurisch et al., 2012). Importantly, the inorganic, clay-bound nitrogen is liberated prior to organic nitrogen and converted to  $\text{N}_2$  due to its lower thermal stability during thermal degradation (Jurisch and Krooss, 2008; Jurisch et al., 2012).

A recent pyrolysis experiment further illustrated that the  $\text{N}_2$  generation from different nitrogen species in shales is primarily controlled by the thermal maturity levels.  $\text{N}_2$  gas is mainly derived from the inorganic silicate-bound nitrogen in the stage of equivalent vitrinite reflectance ( $\text{EqVRo}$ ) < 3.4%, whereas the  $\text{N}_2$  generated from organic nitrogen increases rapidly at higher thermal maturity levels with a maximum  $\text{N}_2$  yields at  $\text{EqVRo} = 4.9\%$  (Gai et al., 2020). Although the thermal maturity of the lower Cambrian shale is generally higher than that of the

Ordovician–Silurian shale (EqVRo values are between 2.0% and 3.0%; review by Nie et al., 2021), its EqVRo values are mostly in the range of 2.0–3.5% (Tian et al., 2015; Liu et al., 2016; Xia et al., 2018), suggesting that the conversion of silicate-bound nitrogen during thermal degradation may have played a major role in the formation of high concentration of N<sub>2</sub> in the lower Cambrian shale reservoirs and that the contribution from organic nitrogen may have been limited. The co-variation between the TN-intercept in bulk rocks and N<sub>2</sub> concentrations in the shale reservoirs (Fig. 5b) further supports that the high abundance of silicate-bound nitrogen in the lower Cambrian shale is likely to be the internal driving factor of N<sub>2</sub> enrichment in shale reservoirs. This scenario is probably responsible for the differential accumulation of N<sub>2</sub> in the overmature lower Cambrian shale and Ordovician–Silurian shale across the Yangtze Block, because the former displays significantly higher proportions of silicate-bound nitrogen than the latter.

The preservation conditions of shale gas may have played an important role in the enrichment of N<sub>2</sub> in the lower Cambrian shale reservoirs as an external factor. On microscopic scales especially in local shale reservoirs with fractures and high permeability, the late-generated N<sub>2</sub> would replace methane in the fractures, resulting in the discharge of methane and reducing its partial pressure, thereby promoting the desorption of methane from the surface of nanopores within organic matter (adsorbed gas) and further discharging methane out of the reservoir (Bustin et al., 2016; Li and Elsworth, 2019). On macroscopic scales, the lower Cambrian N<sub>2</sub>-rich shale gas on the Yangtze Block mostly occurs in regions where deep-seated faults extend to the surface (Su et al., 2019; Wu et al., 2019). In this case, the activity of faults over geologic time may have led to the loss of early generated methane, such that the shale reservoir could be recharged by the late-generated N<sub>2</sub>-rich gas after the fault was sealed (Gai et al., 2020). Indeed, previous investigations have shown that high concentrations of N<sub>2</sub> are generally accompanied by an extremely low overall gas content (< 0.5 m<sup>3</sup>/t) in the lower Cambrian shale reservoirs (Liu et al., 2016; Huang et al., 2019; Wang et al., 2020), suggesting that these shale reservoirs may have experienced long-term methane escape.

In summary, the specific marine redox and biogeochemical nitrogen cycles appear to have resulted in an unusually high abundance of silicate-bound nitrogen in the lower Cambrian shale, which created a higher N<sub>2</sub> generation potential at a certain thermal maturity level (e.g., EqVRo < 3.4%). The high N<sub>2</sub> fraction and the complex geological history would have promoted the desorption and outward loss of methane to various extents, and therefore led to the accumulation of N<sub>2</sub> in ultra-tight shale reservoirs. These N<sub>2</sub>-rich sedimentary reservoirs could have been either exposed to the surface through tectonic uplift or communicated with the surface environment through large-scale faults over long-term geological timescales. The release of this gas could represent a significant nitrogen source flux into the atmosphere that has previously been overlooked.

A previous estimate of the metamorphic nitrogen flux from sedimentary rocks deposited on continental shelves used the corresponding flux of CO<sub>2</sub> from organic carbon metamorphism as a starting point, divided this value by the average C/N ratio of 10 of unmetamorphosed sediments, and then assumed that nitrogen is degassed 1.5–3 times as fast as carbon, based on the observation that C/N ratios increase by a factor of 1.5–3 in greenschist-to-granulite metamorphic rocks (see Stüeken et al., 2016, and references therein). The total nitrogen flux derived from this calculation was thus 0.8–3 × 10<sup>11</sup> mol/yr, which is similar to the total amount

of N buried in marine sediments today and therefore a significant factor in the balance of the global geological N cycle. The atmosphere currently holds  $2.87 \times 10^{20}$  mol N (Johnson and Goldblatt, 2015), meaning that the residence time of N in the atmosphere with respect to its major long-term sources and sinks is on the order of one billion years. Perturbing the atmospheric reservoir is therefore difficult on short timescales; however, it is conceivable that an enhanced N-flux from the metamorphism of clays could have persisted for hundreds of millions of years in the early and late Proterozoic, when productivity was elevated (Crockford et al., 2018) and euxinic conditions are thought to have been more prevalent than today (e.g., Reinhard et al. 2013). The effects may be quantifiable in future studies with more detailed information on the thickness, extent and burial history of source rocks from those time periods.

## 5. Conclusions

Our comprehensive C-N geochemical study of the lower Cambrian shale across the Yangtze Block indicates a spatial trend of excess silicate-bound nitrogen throughout the Yangtze Block, with high abundance at the shelf and slope settings. The anomalously negative  $\delta^{15}\text{N}$  values ( $< -2\text{‰}$ ) provide evidence for widespread partial assimilation of  $\text{NH}_4^+$  in these environments, where the  $\text{NH}_4^+$  concentrations may have accumulated to high levels in the water column and sedimentary pore waters. This excess  $\text{NH}_4^+$  was likely trapped by clay minerals due to the high abundance of illitic clays (illite + illite/smectite mixed-layer) in the lower Cambrian shale, resulting in the observed positive TN-intercepts. Further, the silicate-bound nitrogen in bulk rock shale and the  $\text{N}_2$  concentration in shale reservoir are highly synchronized in spatial variability, indicating that the high proportion of silicate-bound nitrogen in lower Cambrian shale may have played a key role in the formation of  $\text{N}_2$ -rich gas in shale reservoirs. Our work may thus help refine exploration strategies for natural gas reservoirs in the future. Furthermore, we reveal that the metamorphic  $\text{N}_2$  gas flux from the geosphere to the atmosphere is dependent on environmental conditions during sediment deposition, because the anoxic conditions that lead to the accumulation of ammonium in clay minerals may develop into a previously unrecognized source of  $\text{N}_2$  gas into the atmosphere once those sediments undergo burial metamorphism. Ocean redox conditions of the past may therefore set the pace for atmospheric evolution over subsequent 100-Myr-timescales. These effects should be taken into account in future time-resolve estimates of fluxes in the geological nitrogen cycle.

## Acknowledgments

This work was supported by the National Natural Science Foundation of China (42102171, 41927801, 41972132), the Fundamental Research Funds for the Central Universities (2652019098), and the China Scholarship Council (202006405019). EES acknowledges funding from a NERC grant (NE/V010824/1).

## References

- Abdulla, H.A., Burdige, D.J., Komada, T., 2018. Accumulation of deaminated peptides in anoxic sediments of Santa Barbara Basin. *Geochim. Cosmochim. Acta* 223, 245-258.
- Ader, M., Thomazo, C., Sansjofre, P., Busigny, V., Papineau, D., Laffont, R., Cartigny, P., Halverson, G.P., 2016. Interpretation of the nitrogen isotopic composition of Precambrian

- sedimentary rocks: Assumptions and perspectives. *Chem. Geol.* 429, 93-110.
- Altabet, M.A., Francois, R., 1994. Sedimentary nitrogen isotopic ratio as a recorder for surface ocean nitrate utilization. *Glob. Biogeochem. Cycles* 8, 103-116.
- Altabet, M.A., Pilskaln, C., Thunell, R., Pride, C., Sigman, D., Chavez, F., Francois, R., 1999. The nitrogen isotope biogeochemistry of sinking particles from the margin of the Eastern North Pacific. *Deep Sea Res. Part I: Oceanogr. Res. Pap.* 46, 655-679.
- Anbar, A. D., Knoll, A.H., 2002. Proterozoic ocean chemistry and evolution: A bioinorganic bridge? *Science* 297, 1137-1142.
- Behar, F., Gillaizeau, B., Derenne, S., Largeau, C., 2000. Nitrogen distribution in the pyrolysis products of a type II kerogen (Cenomanian, Italy). Timing of molecular nitrogen production versus other gases. *Energy Fuels*. 14, 431-440.
- Boudou, J. P., Espitalie, J., 1995. Molecular nitrogen from coal pyrolysis: Kinetic modelling. *Chem. Geol.* 126, 319-333.
- Boudou, J. P., Schimmelmann, A., Ader, M., Mastalerz, M., Sebito, M., Gengembre, L., 2008. Organic nitrogen chemistry during low-grade metamorphism. *Geochim. Cosmochim. Acta* 72, 1199-1221.
- Boudreau, B. P., Canfield, D. E., 1988. A Provisional Diagenetic Model for Ph in Anoxic Porewaters - Application to the Foam Site. *J. Mar. Res.* 46, 429-455.
- Brewer, P.G., Murray, J. W., 1973. Carbon, nitrogen and phosphorus in the black sea. *Deep-Sea Res. Oceanogr. Abstr.* 20, 803-818.
- Bristow, T. F., Kennedy, M. J., Derkowski, A., Droser, M. L., Jiang, G. Q., Creaser, R. A., 2009. Mineralogical constraints on the paleoenvironments of the Ediacaran Doushantuo Formation. *Proc. Natl. Acad. Sci. U. S. A.* 106, 13190-13195.
- Bustin, A. M. M., Bustin, R. M., Chikatamarla, L., Downey, R., Mansoori, J., 2016. Learnings from a failed nitrogen enhanced coalbed methane pilot: Piceance Basin, Colorado. *Int. J. Coal Geol.* 165, 64-75.
- Calvert, S. E., 2004. Beware intercepts: interpreting compositional ratios in multi-component sediments and sedimentary rocks. *Org. Geochem.* 35, 981-987.
- Canfield, D. E., Glazer, A. N., Falkowski, P. G., 2010. The Evolution and Future of Earth's Nitrogen Cycle. *Science* 330, 192-196.
- Chen, Y., Diamond, C. W., Stüeken, E. E., Cai, C.F., Gill, B. C., Zhang, F.F., Bates, S. M., Chu, X.L., Ding, Y., Lyons, T. W., 2019. Coupled evolution of nitrogen cycling and redoxcline dynamics on the Yangtze Block across the Ediacaran-Cambrian transition. *Geochim. Cosmochim. Acta* 257, 243-265.
- Crockford, P. W., Hayles, J. A., Bao, H., Planavsky, N. J., Bekker, A., Fralick, P. W., Halverson, G. P., Bui, T. H., Peng, Y. Wing, B.A., 2018. Triple oxygen isotope evidence for limited mid-Proterozoic primary productivity. *Nature* 559, 613-616.
- Cui, X., Bustin, R. M., & Dipple, G., 2004. Selective transport of CO<sub>2</sub>, CH<sub>4</sub>, and N<sub>2</sub> in coals: insights from modeling of experimental gas adsorption data. *Fuel*. 83, 293-303.
- Dai, J. X., 1992, Identification and Distinction of Various Alkane Gases. *Sci. China, Ser. B: Chem.* 35, 1246-1257.
- Dai, J. X., Zou, C. N., Liao, S. M., Dong, D. Z., Ni, Y. Y., Huang, J. L., Wu, W., Gong, D. Y., Huang, S. P., Hu, G. Y., 2014. Geochemistry of the extremely high thermal maturity Longmaxi shale gas, southern Sichuan Basin. *Org. Geochem.* 74, 3-12.

- Dang, W., Zhang, J. C., Tang, X., Wei, X. L., Li, Z. M., Wang, C. H., Chen, Q. Liu, C., 2018. Investigation of gas content of organic-rich shale: A case study from Lower Permian shale in southern North China Basin, central China. *Geosci Front.* 9, 559-575.
- Du, Y., Song, H. Y., Tong, J. N., Algeo, T. J., Li, Z., Song, H. J., Huang, J. D., 2021. Changes in productivity associated with algal-microbial shifts during the Early Triassic recovery of marine ecosystems. *Geol. Soc. Am. Bull.* 133, 362-378.
- Feng, L., Li, C., Huang, J., Chang, H., Chu, X., 2014. A sulfate control on marine mid-depth euxinia on the early Cambrian (ca. 529-521 Ma) Yangtze platform, South China. *Precambrian Res.* 246, 123-133.
- Freudenthal, T., Wagner, T., Wenzhöfer, F., Zabel, M., Wefer, G., 2001. Early diagenesis of organic matter from sediments of the eastern subtropical Atlantic: evidence from stable nitrogen and carbon isotopes. *Geochim. Cosmochim. Acta* 65, 1795-1808.
- Fulton, J. M., Arthur, M. A., Freeman, K. H., 2012. Black Sea nitrogen cycling and the preservation of phytoplankton  $\delta^{15}\text{N}$  signals during the Holocene. *Global Biogeochem. Cycles.* 26, GB2030–GB2044.
- Gai, H. F., Tian, H., Cheng, P., He, C. M., Wu, Z. J., Ji, S., Xiao, X. M., 2020. Characteristics of molecular nitrogen generation from overmature black shales in South China: Preliminary implications from pyrolysis experiments. *Mar. Pet. Geol.* 120, 104527.
- Gao, P., Li, S. J., Lash, G. G., Yan, D. T., Zhou, Q., Xiao, X. M., 2021. Stratigraphic framework, redox history, and organic matter accumulation of an Early Cambrian intraplatfrom basin on the Yangtze Platform, South China. *Mar. Pet. Geol.* 130, 105095.
- Heim, S., Jurisch, S., Krooss, B., Weniger, P., Littke, R., 2012. Systematics of pyrolytic  $\text{N}_2$  and  $\text{CH}_4$  release from peat and coals of different thermal maturity. *Int. J. Coal Geol.* 89, 84-94.
- Hoch, M.P., Fogel, M.L., Kirchman, D.L., 1992. Isotope fractionation associated with ammonium uptake by a marine bacterium. *Limnol. Oceanogr.* 37, 1447-1459.
- Houlton, B. Z., Morford, S. L., Dahlgren, R. A., 2018. Convergent evidence for widespread rock nitrogen sources in Earth's surface environment. *Science* 360, 58-62.
- Huang, Y.Z., Zhang, K., Jiang, Z.X., Song, Y., Jiang, S., Jia, C.Z., Liu, W.W., Wen, M., Xie, X.L., Liu, T.L., Li, X., Wang, X., 2019. A cause analysis of the high-content nitrogen and low-content hydrocarbon in shale gas: a case study of the early Cambrian in Xiuwu Basin, Yangtze region. *Geofluids.* 2019.
- Jenden, P. D., Kaplan, I. R., Poreda, R. J., Craig, H., 1988. Origin of Nitrogen-Rich Natural Gases in the California Great Valley - Evidence from Helium, Carbon and Nitrogen Isotope Ratios. *Geochim. Cosmochim. Acta* 52, 851-861.
- Jiang, G. Q., Wang, X. Q., Shi, X. Y., Xiao, S. H., Zhang, S. H., Dong, J., 2012. The origin of decoupled carbonate and organic carbon isotope signatures in the early Cambrian (ca. 542-520 Ma) Yangtze platform. *Earth Planet. Sci. Lett.* 317, 96-110.
- Jin, C. Li, S., C., Algeo, T. J., Planaysky, N. J., Cui, H., Yang, X. L., Zhao, Y. L., Zhang, X. L., Xie, S. C., 2016. A highly redox-heterogeneous ocean in South China during the early Cambrian (similar to 529-514 Ma): Implications for biota-environment co-evolution. *Earth Planet. Sci. Lett.* 441, 38-51.
- Johnson, B., Goldblatt, C., 2015. The nitrogen budget of Earth. *Earth-Sci. Rev.* 148, 150-173.
- Jurisch, A., Krooss, B. M., 2008. A pyrolytic study of the speciation and isotopic composition

- of nitrogen in carboniferous shales of the North German Basin. *Org. Geochem.* 39, 924-928.
- Jurisch, S., Heim, S., Krooss, B., Littke, R., 2012. Systematics of pyrolytic gas (N<sub>2</sub>, CH<sub>4</sub>) liberation from sedimentary rocks: Contribution of organic and inorganic rock constituents. *Int. J. Coal Geol.* 89, 95-107.
- Kartal, B., Kuypers, M. M. M., Lavik, G., Schalk, J., Camp, H. J. M. O. den., Jetten, M. S. M., Strous, M., 2007. Anammox bacteria disguised as denitrifiers: nitrate reduction to dinitrogen gas via nitrite and ammonium. *Environ. Microbiol.* 9, 635-642.
- Kenrick, P., Crane, P. R., 1997. The origin and early evolution of plants on land. *Nature* 389, 33-39.
- Knauer, G.A., Martin, J.H., Bruland, K.W., 1979. Fluxes of particulate carbon, nitrogen, and phosphorus in the upper water column of the northeast Pacific. *Deep-Sea Research* 26, 97-108.
- Koehler, M. C., Stüeken, E. E., Hillier, S., Prave, A. R., 2019. Limitation of fixed nitrogen and deepening of the carbonate-compensation depth through the Hirnantian at Dob's Linn, Scotland. *Palaeogeogr. Palaeoclimatol. Palaeoecol.* 534, 109321.
- Kříbek, B., Sýkorová, I., Pašava, J., Machovič, V., 2007. Organic geochemistry and petrology of barren and Mo-Ni-PGE mineralized marine black shales of the Lower Cambrian Niutitang Formation (South China). *Int. J. Coal Geol.* 72, 240-256.
- Krooss, B. M., Littke, R., Muller, B., Frielingsdorf, J., Schwochau, K., Idiz, E. F., 1995. Generation of nitrogen and methane from sedimentary organic matter: Implications on the dynamics of natural gas accumulations. *Chem. Geol.* 126, 291-318.
- Lam, P., Kuypers, M.M.M., 2011. Microbial nitrogen cycling processes in oxygen minimum zones. *Mar. Sci. Ann. Rev.* 3, 317-345.
- Lam, P., Lavik, G., Jensen, M.M., van de Vossenberg, J., Schmid, M., Woebken, D., Dimitri Gutiérrez, D., Amann, R., Jetten, M.S.M., Kuypers, M.M.M., 2009. Revising the nitrogen cycle in the Peruvian oxygen minimum zone. *Proc. Natl. Acad. Sci. U. S. A.* 106, 4752-4757.
- Li L., Bebout G. E., 2005. Carbon and nitrogen geochemistry of sediments in the Central American convergent margin: Insights regarding subduction input fluxes, diagenesis, and paleoproductivity. *J. Geophys. Res.: Solid Earth* 110, B11202.
- Li, C., Jin, C. S., Planavsky, N. J., Algeo, T. J., Cheng, M., Yang, X. L., Zhao, Y. L., Xie, S. C., 2017. Coupled oceanic oxygenation and metazoan diversification during the early-middle Cambrian?. *Geology.* 45, 743-746.
- Li, Z., D. Elsworth., 2019. Controls of CO<sub>2</sub>-N<sub>2</sub> gas flood ratios on enhanced shale gas recovery and ultimate CO<sub>2</sub> sequestration. *J. Pet. Sci. Eng.* 179, 1037-1045.
- Li, Z., Zhang, J.C., Gong, D.J., Tan, J.Q., Liu, Y., Wang, D.S., Li, P., Tong, Z.Z., Niu, J.L., 2020. Gas-bearing property of the Lower Cambrian Niutitang Formation shale and its influencing factors: A case study from the Cengong block, northern Guizhou Province, South China. *Mar. Pet. Geol.* 120, 104556.
- Littke, R., Krooss, B., Idiz, E., Frielingsdorf, J., 1995. Molecular Nitrogen in Natural-Gas Accumulations - Generation from Sedimentary Organic-Matter at High-Temperatures. *AAPG Bull.* 79, 410-430.
- Liu, Q., Jin, Z. J., Chen, J. F., Krooss, B. M., Qin, S. F., 2012. Origin of nitrogen molecules in

- natural gas and implications for the high risk of N<sub>2</sub> exploration in Tarim Basin, NW China. *J. Pet. Sci. Eng.* 81, 112-121.
- Liu, Y., Magnall, J. M., Gleeson, S. A., Bowyer, F., Poulton, S. W., Zhang, J. C., 2020. Spatio-temporal evolution of ocean redox and nitrogen cycling in the early Cambrian Yangtze ocean. *Chem. Geol.* 554, 119803.
- Liu, Y., Zhang, J. C., Ren, J., Liu, Z. Y., Huang, H., Tang, X., 2016. Stable isotope geochemistry of the nitrogen-rich gas from lower Cambrian shale in the Yangtze Gorges area, South China. *Mar. Pet. Geol.* 77, 693-702.
- Liu, Z. Y., Chen, D. X., Zhang, J. C., Lv, X. X., Dang, W., Liu, Y., Liao, W. H., Li, J. H., Wang, Z. Y., Wang, F. W., 2019. Combining Isotopic Geochemical Data and Logging Data to Predict the Range of the Total Gas Content in Shale: A Case Study from the Wufeng and Longmaxi Shales in the Middle Yangtze Area, South China. *Energy Fuels.* 33, 10487-10498.
- Luo, G.M., Algeo, T. J. Zhan, R. B., Yan, D.T., Huang, J. H., Liu, J.S., Xie, S.C., 2016. Perturbation of the marine nitrogen cycle during the Late Ordovician glaciation and mass extinction. *Palaeogeogr. Palaeoclimatol. Palaeoecol.* 448, 339-348.
- Ma, Y., Zhong, N. N., Yao, L. P., Huang, H. P., Larter, S., Jiao, W. W., 2020. Shale gas desorption behavior and carbon isotopic variations of gases from canister desorption of two sets of gas shales in south China. *Mar. Pet. Geol.* 113, 104127.
- Michiels, C.C., Darchambeau, F., Roland, F.A.E., Morana, C., Lliros, M., Garcia-Armisen, T., Thamdrup, B., Borges, A.V., Canfield, D.E., Servais, P., Descy, J.P., Crowe, S.A., 2017. Iron-dependent nitrogen cycling in a ferruginous lake and the nutrient status of Proterozoic oceans. *Nat. Geosci.* 10, 217-U176.
- Müller, P., 1977. CN ratios in Pacific deep-sea sediments: Effect of inorganic ammonium and organic nitrogen compounds sorbed by clays. *Geochim. Cosmochim. Acta* 41, 765-776.
- Muzuka, A.N.N., Hillaire-Marcel, C., 1999. Burial rates of organic matter along the eastern Canadian margin and stable isotope constraints on its origin and diagenetic evolution. *Mar. Geol.* 160, 251-270.
- Nie, H. K., Chen, Q., Zhang, G. R., Sun, C. X., Wang, P. W., Lu, Z. Y., 2021. An overview of the characteristic of typical Wufeng–Longmaxi shale gas fields in the Sichuan Basin, China. *Nat. Gas Ind B.* 8, 217-230.
- Pecharsky, V., Zavalij, P., 2003. *Fundamentals of Powder Diffraction and Structural Characterization of Minerals.* Kluwer Academic Publishers. New York, pp. 713.
- Reinhard, C. T., Planavsky, N. J., Robbins, L. J., Partin, C. A., Gill, B. C., Lalonde, S. V., Bekker, A., Konhauser, K. O. Lyons, T. W., 2013. Proterozoic ocean redox and biogeochemical stasis. *Proc. Natl. Acad. Sci. U. S. A.* 110, 5357-5362.
- Schroeder, P. A., McLain, A. A., 1998. Illite-smectites and the influence of burial diagenesis on the geochemical cycling of nitrogen. *Clay Miner.* 33, 539-546.
- Sigman, D.M., Karsh, K.L., Casciotti, K.L., 2009. Nitrogen isotopes in the ocean. In: Steele, J.H., Thorpe, S.A., Turekian, K.K. (Eds.), *Encyclopedia of Ocean Sciences.* Academic Press, Oxford, pp. 40-54.
- Sørensen, J., 1978. Capacity for denitrification and reduction of nitrate to ammonia in a coastal marine sediment. *Applied and Environ. Microbiol.* 35, 301-305.
- Steiner, M., Li, G. X., Qian, Y., Zhu, M. Y., Erdtmann, B.-D., 2007. Neoproterozoic to early

- Cambrian small shelly fossil assemblages and a revised biostratigraphic correlation of the Yangtze Platform (China). *Palaeogeogr. Palaeoclimatol. Palaeoecol.* 254, 67-99.
- Stüeken, E. E., Kipp, M. A., Koehler, M. C., Buick, R., 2016. The evolution of Earth's biogeochemical nitrogen cycle. *Earth-Sci. Rev.* 160, 220-239.
- Stüeken, E. E., Zaloumis, J., Meixnerova, J., Buick, R., 2017. Differential metamorphic effects on nitrogen isotopes in kerogen extracts and bulk rocks. *Geochim. Cosmochim. Acta* 217, 80-94.
- Su, Y., Wang, W., Li, J., Gong, D., F. Shu., 2019. Origin of nitrogen in marine shale gas in Southern China and its significance as an indicator. *Oil Gas Geol.* 40, 1185-1196.
- Thunell, R.C., Sigman, D.M., Muller-Karger, F., Astor, Y., Varela, R., 2004. Nitrogen isotope dynamics of the Cariaco Basin, Venezuela. *Global Biogeochem. Cycl.* 18, GB3001.
- Tian, H., Pan, L., Zhang, T. W., Xiao, X. M., Meng, Z. P., Huang, B. J., 2015. Pore characterization of organic-rich Lower Cambrian shales in Qiannan Depression of Guizhou Province, Southwestern China. *Mar. Pet. Geol.* 62, 28-43.
- Wang, S., 2018. Shale gas exploitation: Status, problems and prospect. *Nat. Gas Ind B.* 5, 60-74.
- Wang, X., Jiang, Z. X., Zhang, K., Wen, M., Xue, Z. X., Wu, W., Huang, Y. Z., Wang, Q. Y., Liu, X. X., Liu, T. L., Xie, X. L., 2020. Analysis of Gas Composition and Nitrogen Sources of Shale Gas Reservoir under Strong Tectonic Events: Evidence from the Complex Tectonic Area in the Yangtze Plate. *Energies.* 13, 281.
- Wu, Y. W., Gong, D.J., Li, T. F., Wang, X., Tian, H., 2019. Distribution characteristics of nitrogen-bearing shale gas and prospective areas for exploration in the Niutitang Formation in the Qianzhong uplift and adjacent areas. *Geochimica.* 48, 613-623 ( in Chinese with English abstract).
- Xia, P., Wang, G.L., Zeng, F. G., Mou, Y. L., Zhang, H. T., Liu, J.G., 2018. The characteristics and mechanism of high-over matured nitrogen-rich shale gas of Niutitang Formation, northern Guizhou area. *Nat Gas Geosci.* 29, 1345-1355.
- Zerkle, A., Junium, C.K., Canfield, D.E., House, C.H., 2008. Production of <sup>15</sup>N-depleted biomass during cyanobacterial N<sub>2</sub>-fixation at high Fe concentrations. *J. Geophys. Res.: Biogeosci.* 113, 112-118.
- Zhang, X., Sigman, D.M., Morel, F.M., Kraepiel, A.M., 2014. Nitrogen isotope fractionation by alternative nitrogenases and past ocean anoxia. *Proc. Natl. Acad. Sci.* 111, 4782-4787.
- Zhao, J. H., Jin, Z. J., Hu, Q. H., Liu, K. Y., Liu, G. X., Gao, B., Liu, Z. B., Zhang, Y. Y., Wang, R. Y., 2019. Geological controls on the accumulation of shale gas: A case study of the early Cambrian shale in the Upper Yangtze area. *Mar. Pet. Geol.* 107, 423-437.
- Zhu, M. Y., Strauss H. Shields G. A., 2007. From snowball earth to the Cambrian bioradiation: calibration of Ediacaran-Cambrian earth history in South China. *Palaeogeogr. Palaeoclimatol. Palaeoecol.* 254, 1-6.
- Zhu, M. Y., Zhang, J. M., Steiner, M., Yang, A. H., Li, G. X., Erdtmann, B. D., 2003. Sinian-Cambrian stratigraphic framework for-shallow- to deep-water environments of the Yangtze Platform: an integrated approach. *Prog Nat Sci-Mater.* 13, 951-960.
- Zhu, Y. N., Shi, B. Q., Fang, C. B., 2000. The isotopic compositions of molecular nitrogen: implications on their origins in natural gas accumulations. *Chemi Geol.* 164, 321-330.
- Zou, C. N., Yang, Z., Dai, J. X., Dong, D. Z., Zhang, B. M., Wang, Y. M., Deng, S. H., Huang,

J. Q., Liu, K. Y. Yang, C. Wei, G. Q., Pan, S. Q., 2015. The characteristics and significance of conventional and unconventional Sinian-Silurian gas systems in the Sichuan Basin, central China. *Mar. Pet. Geol.* 64, 386-402.

## Figures

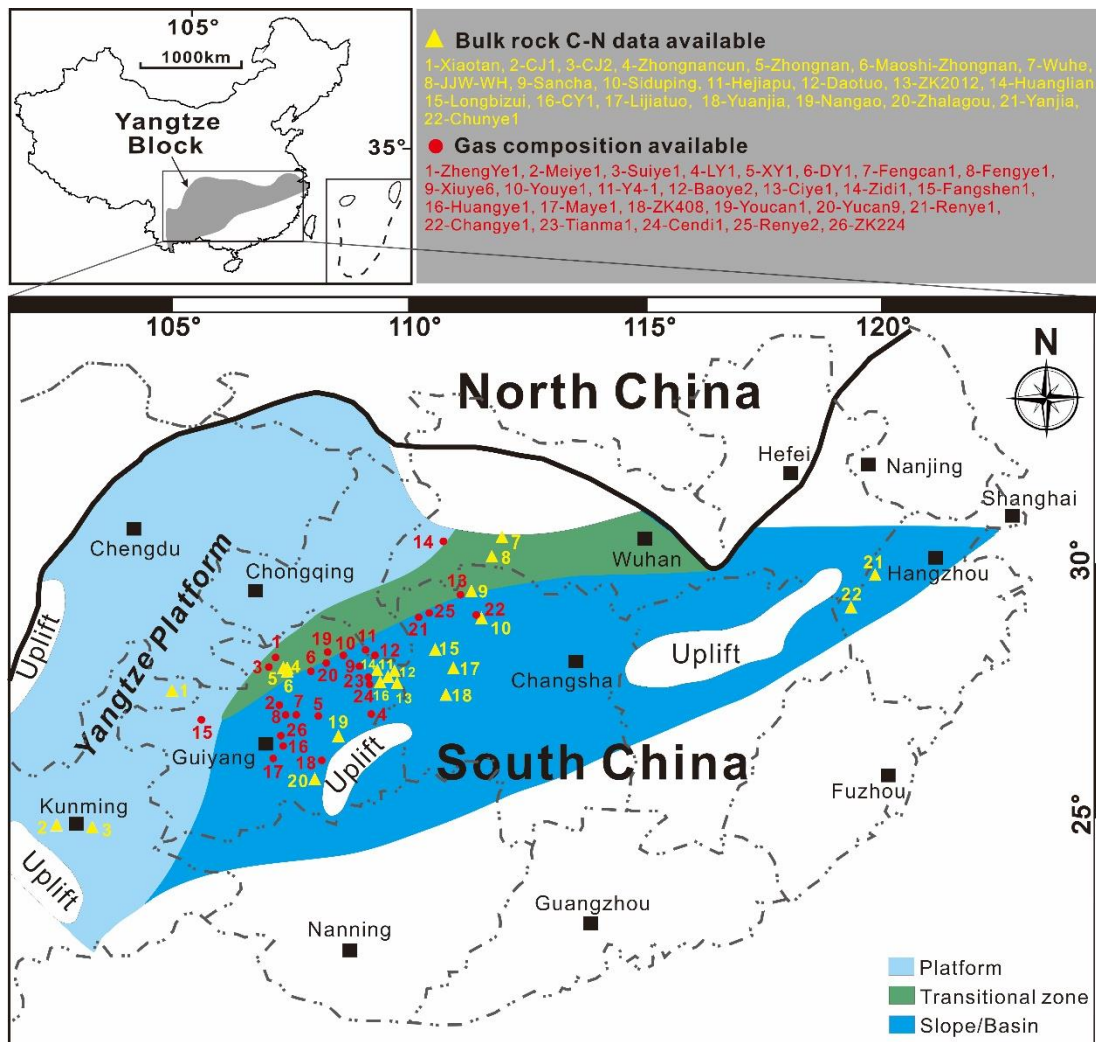


**Figure 1.** Tectonic setting and simplified Paleogeographic map of the Yangtze Block during the early Cambrian (modified after Jiang et al., 2012).

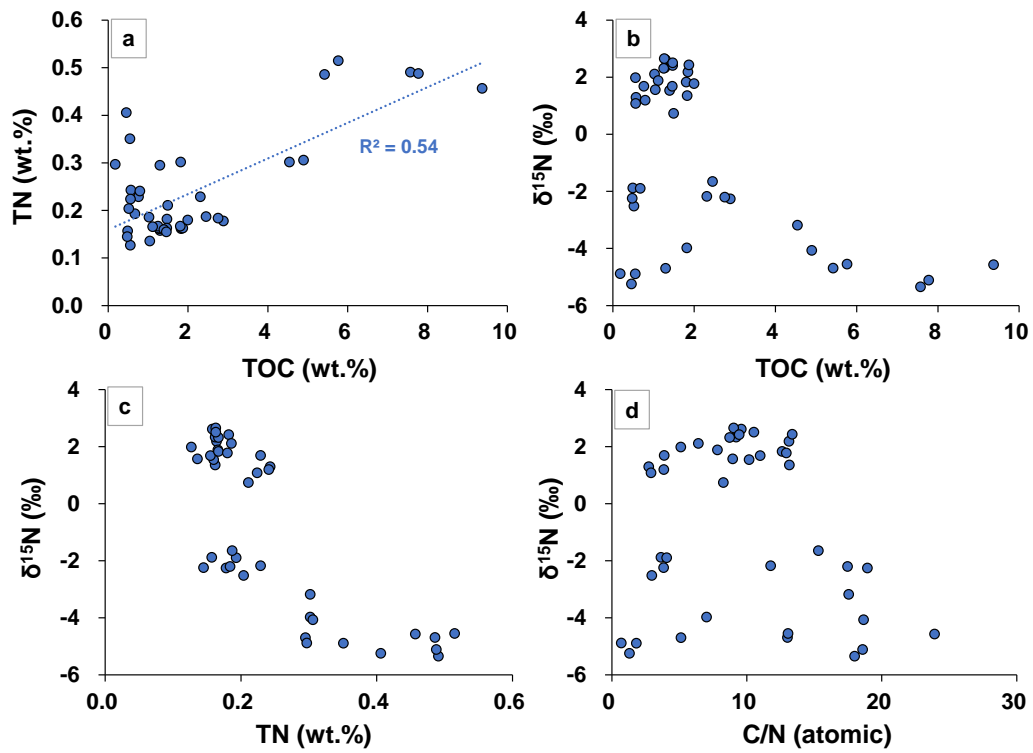


**Figure 2.** Crossplots of TN versus TOC (a),  $\delta^{15}\text{N}_{\text{sed}}$  versus TOC (b),  $\delta^{15}\text{N}_{\text{sed}}$  versus TN (c) and  $\delta^{15}\text{N}_{\text{sed}}$  versus C/N (d). Data are from the CY 1 well of this study.

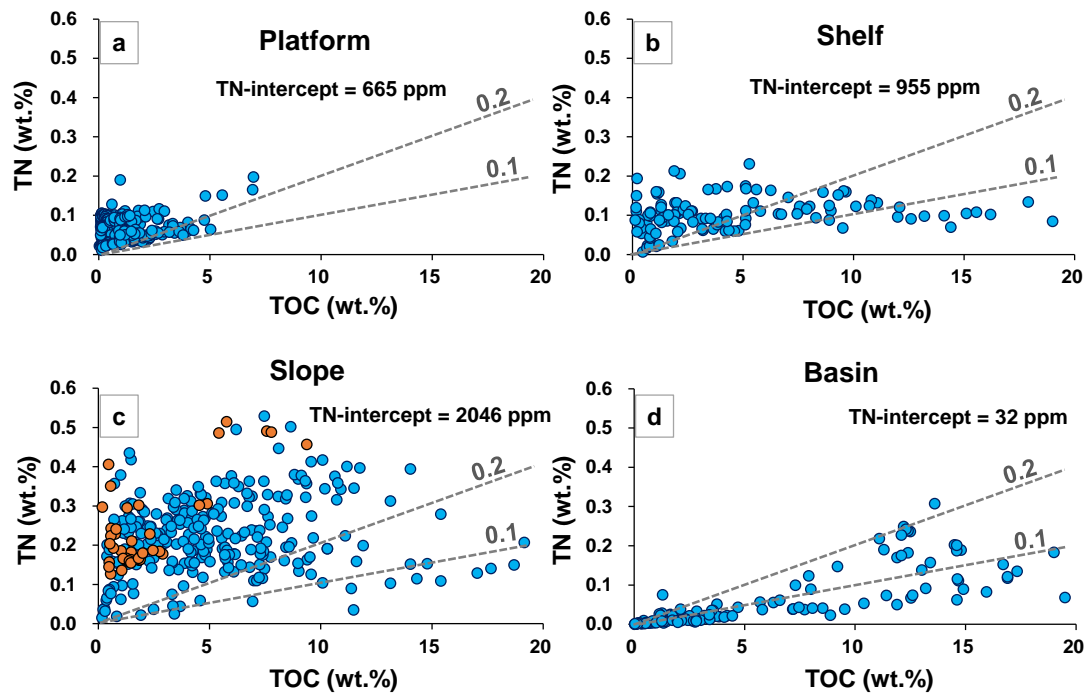


**Figure 3.** Cross plots of TOC versus TN from platform (a), shelf (b), slope (c) and basin (d) successions across the Yangtze Block. The data includes only samples from the intervals of lower Cambrian shale target (~526–515 Ma). The orange dots represent the data from this study and the blue dots represent the compiled data from the Yangtze Block. The positive intercept on the TN axis indicates the average excess silicate-bound nitrogen concentration. The dotted lines represent the TN/TOC ratios (0.01 to 0.02) of coal or kerogen.

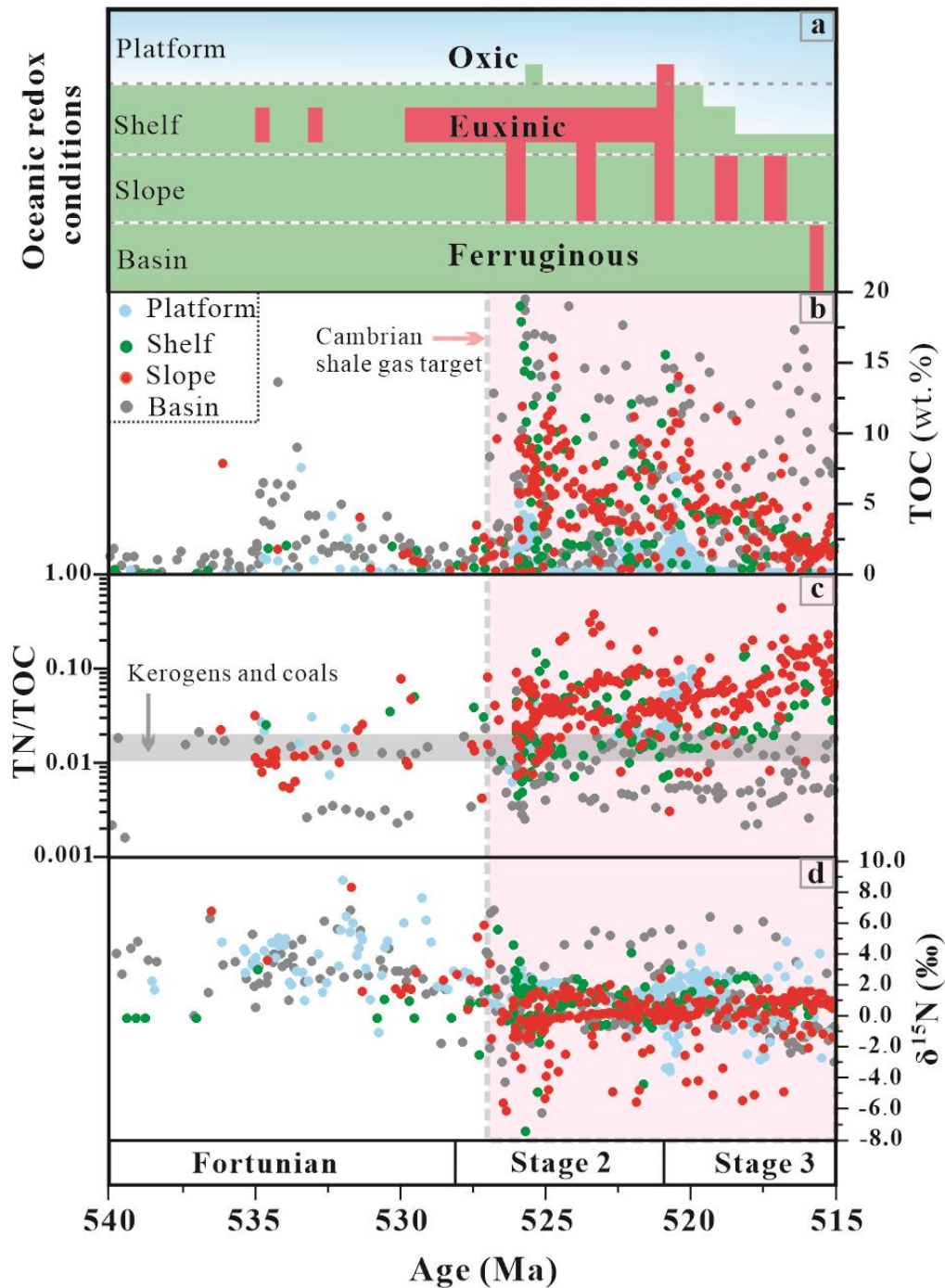


**Figure 4.** (a) Schematic evolution of ocean redox conditions in South China based on iron speciation data (Jin et al., 2016; Li et al., 2017; Liu et al., 2020, and references therein). (b) Long term TOC variations from Fortunian to Cambrian Stage 3 (~540–515 Ma) in South China. (c) Long term TN/TOC variations from Fortunian to Cambrian Stage 3 in South China. (d) Long term  $\delta^{15}\text{N}$  variations from Fortunian to Cambrian Stage 3 in South China. The pink area indicates the Cambrian shale gas target (~526–515 Ma) in South China.

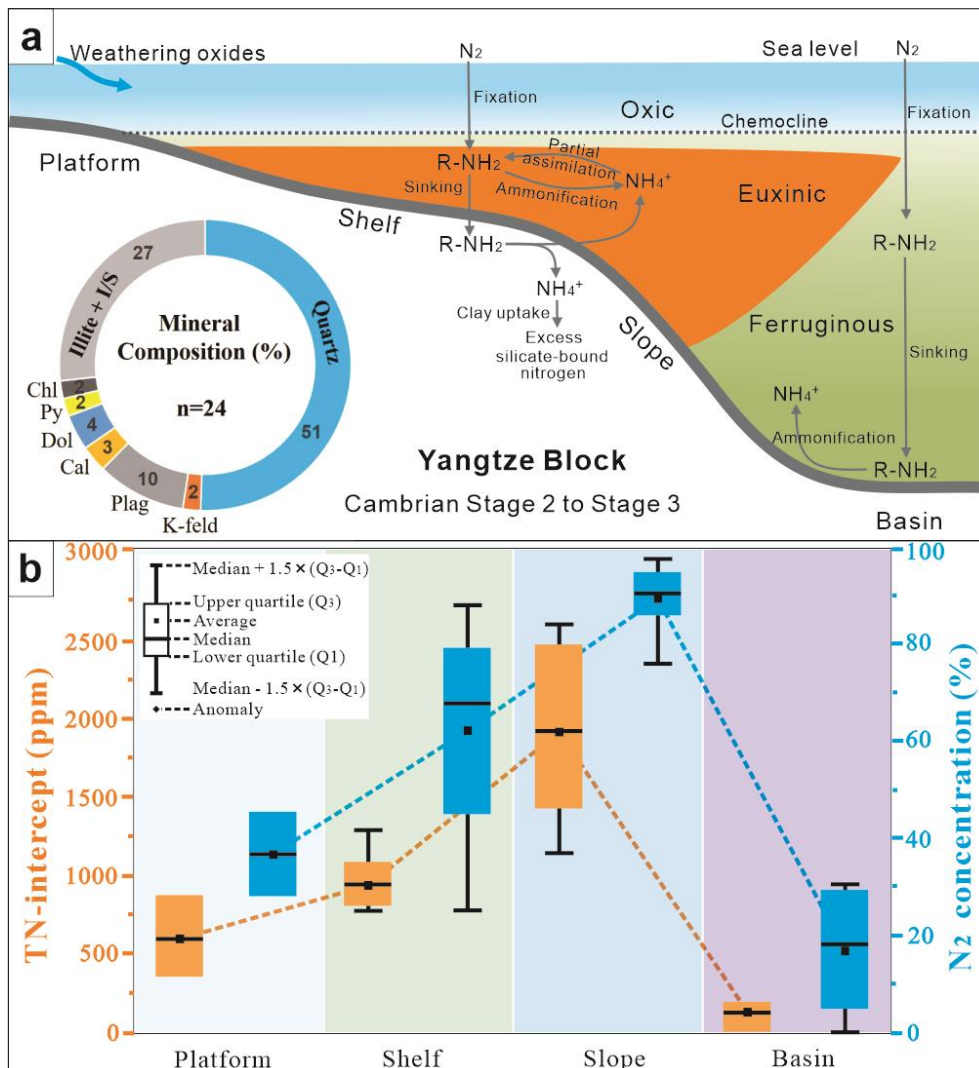


**Figure 5.** (a) Schematic diagram of the marine nitrogen cycle during Cambrian Stage 2 to early Stage 3 in South China, and the donut chart represents the average mineral composition ( $n = 24$ ) of the lower Cambrian shales across the Yangtze Block. (b) Box and whisker plots of positive TN-intercept values in bulk rock shale and the N<sub>2</sub> concentrations in shale reservoir from different paleogeographic environments on the Yangtze Block.